Scanning Gate Microscopy of a Nanostructure where Electrons Interact

Axel Freyn, Ioannis Kleftogiannis, Jean-Louis Pichard

▶ **To cite this version:**

Axel Freyn, Ioannis Kleftogiannis, Jean-Louis Pichard. Scanning Gate Microscopy of a Nanostructure where Electrons Interact. Physical Review Letters, 2008, 100, pp.226802-1. 10.1103/PhysRevLett.100.226802 . hal-00218234v2

HAL Id: hal-00218234
https://hal.science/hal-00218234v2

Submitted on 7 Oct 2008

HAL is a multi-disciplinary open access archive for the deposit and dissemination of scientific research documents, whether they are published or not. The documents may come from teaching and research institutions in France or abroad, or from public or private research centers.

L'archive ouverte pluridisciplinaire **HAL**, est destinée au dépôt et à la diffusion de documents scientifiques de niveau recherche, publiés ou non, émanant des établissements d'enseignement et de recherche français ou étrangers, des laboratoires publics ou privés.

Scanning Gate Microscopy of a Nanostructure where Electrons Interact

Axel Freyn, Ioannis Kleftogiannis,* and Jean-Louis Pichard
Service de Physique de l'État Condensé (CNRS URA 2464), DSM/IRAMIS/SPEC, CEA Saclay, 91191 Gif-sur-Yvette Cedex, France

We show that scanning gate microscopy can be used for probing electron-electron interactions inside a nanostructure. We assume a simple model made of two non interacting strips attached to an interacting nanosystem. In one of the strips, the electrostatic potential can be locally varied by a charged tip. This change induces corrections upon the nanosystem Hartree-Fock self-energies which enhance the fringes spaced by half the Fermi wave length in the images giving the quantum conductance as a function of the tip position.

PACS numbers: 07.79.-v,71.10.-w,72.10.-d,73.23.-b

Semiconductor nanostructures based on two dimensional electron gases (2DEGs) have been extensively studied, with the expectation of developing future devices for sensing, information processing and quantum computation. Scanning gate microscopy (SGM) consists in using the charged tip of an AFM cantilever as a movable gate for studying these nanostructures. A typical SGM setup is sketched in FIG. 1. A negatively charged tip capacitively couples with the 2DEG at a distance r_T from the nanostructure, creating a small depletion region that scatters the electrons. Scanning the tip around the nanostructure and measuring the quantum conductance g between two ohmic contacts put on each side of the nanostructure as a function of the tip position provide the SGM images. If the nanostructure is a quantum point contact (QPC), the charged tip can reduce [1] g by a significant fraction $\delta g = g - g_0$, when the conductance without tip g_0 is biased on the first conductance plateau $g_q = 2e^2/h$. Moreover, fringes spaced by $\lambda_F/2$, half the Fermi wave length, and falling off with distance r_T from the QPC, can be seen in the experimental images giving δg as a function of the tip position. Very small distances r_T were not scanned in Refs. [1, 2], but this was done [3] later, giving extra ring structures inside the QPC if g_0 is biased between the conductance plateaus. Scanning gate microscopy has been recently used for studying QPCs [4], open quantum rings [5] and quantum dots created in carbon nanotubes [6] and 2DEGs [7].

Many features of the observed SGM images can be described by single particle theories [5, 8, 9]. However, many body effects are expected to be important inside certain nanostructures (almost closed QPC around the $0.7(2e^2/h)$ conductance anomaly [10], quantum dots of low electron density). We show in this letter that these many body effects can be observed in the SGM images of such nanostructures. Two main signatures of the interaction are identified: fringes of enhanced magnitude, falling off as $1/r_T^2$ near the nanostructure, before falling off as $1/r_T$ far from the nanostructure, and a phase shift of the fringes between these two regions. Though we study this interaction effect using a very simple model, our theory can be extended to any nanostructure inside which electrons interact.

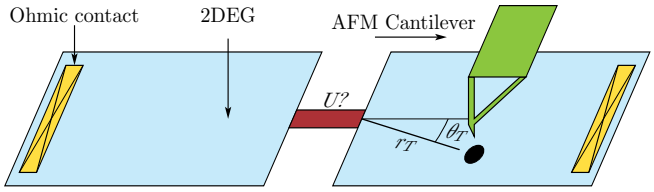

FIG. 1: Scheme of a SGM setup: Two 2DEGs are connected via a nanostructure (red). The negatively (positively) charged tip creates a small depletion (accumulation) region (•) which scatters electrons in the right 2DEG. By scanning the tip and measuring the quantum conductance g between the 2 ohmic contacts, one can detect the interaction U acting inside the nanostructure.

Without interaction, the nanostructure and the depletion region created by the tip are independent scatterers. With interactions inside the nanostructure, the effective nanostructure transmission becomes non local and can be modified by the tip. The origin of this non local effect is easy to explain [11, 12, 13] if one uses the Hartree-Fock (HF) approximation. The tip induces Friedel oscillations of the electron density, which can modify the density inside the nanostructure. As one moves the tip, this changes the Hartree corrections of the nanostructure. A similar effect changes also the Fock corrections [11, 12, 13]. When the electrons do not interact inside the nanostructure, the SGM images probe the interferences of electrons which are transmitted by the nanostructure and elastically backscattered by the tip at the Fermi energy E_F. When the electrons interact inside the nanostructure, the information given by the SGM images becomes more complex, since the scattering processes of energies below E_F influence also the quantum conductance. In the HF approximation, these non local processes taking place at all energies below E_F are taken into account by the integral equations giving the nanosystem HF corrections.

The principle for the detection of the interaction U via SGM can be simply explained in one dimension, when the strips are semi-infinite chains. If $U = 0$, the trans-

mitted flow interferes with the flow reflected by the tip, giving rise to Fabry-Pérot oscillations which do not decay as $r_T \to \infty$. Hence the conductance g of a nanostructure in series with a tip exhibits oscillations which do not decay when r_T increases. If $U \neq 0$, the HF-corrections of the nanostructure are modified by the Friedel oscillations induced by the tip inside the nanostructure. This gives an additional effect for g, which decays as the Friedel oscillations causing it ($1/r_T$-decay in 1d, with oscillations of period $\lambda_F/2$). Measuring g as a function of the tip position, one gets oscillations of period $\lambda_F/2$ in the two cases, but their decays are different and allow to measure the interaction strength U inside the nanosystem.

Interactions in 1d chains give rise to a Luttinger-Tomonaga liquid and cannot be neglected. It is necessary to take 2d strips of sufficient electron density (small factor r_s) for neglecting interaction outside the nanosystem. The effect of the tip becomes more subtle with 2d strips: First, the Friedel oscillations decreasing as $1/r^d$ in d dimensions, the effect of the tip upon g has a faster decay, unless focusing effects take place. Second, the non interacting limit becomes more complicated. The probability for an electron of energy E_F to reach the tip, and to be reflected through the nanostructure also decays as $r_T \to \infty$. Assuming isotropy, the probabilities of these two events should decay as $1/r_T$, giving a total $1/r_T^2$ decay for g. But isotropy is not a realistic assumption for SGM setups. The transmission can be strongly focused, making the effect of the tip a function of the angle θ_T. Spectacular focusing effects have been observed [2] using a QPC: The effect of the tip is mainly focused around $\theta_T \approx 0$ or $\pm\pi/4$, depending if $g_0 \approx g_q$ or $2g_q$.

For studying SGM with 2d strips more precisely, we use a simple model sketched in FIG. 2 (left), assuming spin polarized electrons (spinless fermions). The Hamiltonian reads $H = H_{\rm nano} + H_{\rm strips} + H_T$. For the nanostructure, we take a nanosystem with two sites of energy V_G and of hopping term t_d. For the interaction, we take a repulsion of strength U between these two sites. We assume that V_G can be varied by an external gate. The Hamiltonian of the nanosystem reads

$$H_{\rm nano} = V_G \sum_{x=0}^{1} n_{x,0} - t_d(c^\dagger_{0,0}c_{1,0} + H.c.) + U n_{0,0}n_{1,0}. \quad (1)$$

$c_{x,y}$ ($c^\dagger_{x,y}$) is the annihilation (creation) operator at site x, y, and $n_{x,y} = c^\dagger_{x,y}c_{x,y}$.

$$H_{\rm strips} = -t_{\rm h} \sum_{x,y} (c^\dagger_{x,y}c_{x,y+1} + c^\dagger_{x,y}c_{x+1,y} + H.c.) \quad (2)$$

describes the strips and their couplings to the nanosystem (see FIG. 2 (left)). We assume hard wall boundaries in the y-direction. $t_{\rm h} = 1$ sets the energy scale. The depletion (accumulation) region created by a negatively (positively) charged tip located on top of a site of coordinates $(x_T > 1, y_T) = r_T(\cos\theta_T, \sin\theta_T)$ is described by a local Hamiltonian $H_T = V_T n_{x_T,y_T}$.

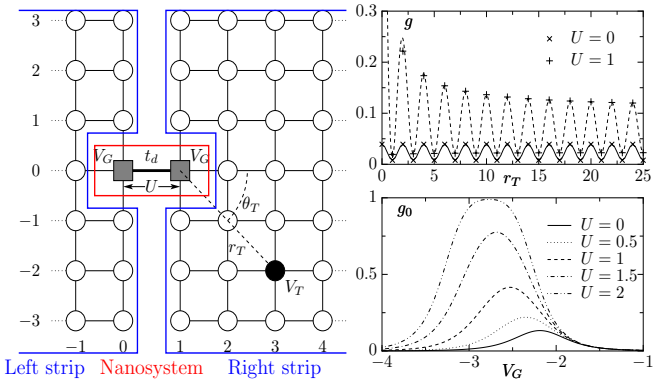

FIG. 2: Left: Used model: 2 strips of width $2L_y + 1$ (here $L_y = 3$) are connected via a nanosystem (2 sites ■, hopping t_d and potentials V_G). The repulsion U acts only inside the nanosystem. The charged tip gives rise to a potential V_T (•) at a distance r_T from the nanosystem. Upper right: SGM measure using 1d chains ($L_y = 0$) at half-filling ($k_F = \pi/2$). The conductance g of the nanosystem ($V_G = -U/2$ and $t_d = 0.1$) in series with a tip ($V_T = 2$) is given as a function of r_T. Fits $0.024 + 0.016\cos(\pi r_T)$ (solid line) and $0.066 + 0.132/r_T + (0.043 + 0.014/r_T)\cos(\pi r_T)$ (dashed line). Lower right: Conductance g_0 without tip ($V_T = 0$) as a function of V_G for 2d strips ($2L_y + 1 = 301$). $E_F = -3.57$ ($k_F = 0.668$), $t_d = 0.1$ and different values of U.

In FIG. 2 (upper right), we show how to detect U by scanning gate microscopy in the 1d limit of our model ($L_y = 0$). The chains are half-filled ($E_F = 0$), and the conductance g of the nanosystem in series with a tip is given as a function of r_T. If $U = 0$, g exhibits even-odd oscillations of constant amplitude, while these oscillations fall off as $1/r_T$ near the nanosystem if $U \neq 0$. When $L_y = 0$, the HF corrections can be obtained using an extrapolation method [11, 12, 13]. When L_y is large, using self-energies becomes more efficient for calculating the HF corrections and the conductance g.

The retarded ($z = E + i\eta$) and advanced ($z = E - i\eta$) Green's functions of the nanosystem at an energy E, $\eta \to 0^+$ are given by the 2×2-matrix

$$G_{\rm nano} = \begin{pmatrix} z - V_G - \sigma_{\mathbf{0}} - \Sigma^{\rm H}_{\mathbf{0}} & t_d - \Sigma^{\rm F} \\ t_d - \Sigma^{\rm F} & z - V_G - \sigma_{\mathbf{1}} - \Sigma^{\rm H}_{\mathbf{1}} \end{pmatrix}^{-1}. \quad (3)$$

The self-energies $\sigma_{\mathbf{0}}$ and $\sigma_{\mathbf{1}}$ describe the couplings of the left and right strips to the nanosystem sites $\mathbf{0} = (0,0)$ and $\mathbf{1} = (1,0)$ respectively. If $G^{L,R}_{\rm strip}$ are the Green's functions of the two strips excluding the 2 nanosystem sites, one gets

$$\sigma_{\mathbf{0}} = \textstyle\sum_{I,J} \langle I|G^L_{\rm strip}|J\rangle \quad (4)$$

$$\sigma_{\mathbf{1}} = \textstyle\sum_{I,J} \langle I|G^R_{\rm strip}|J\rangle. \quad (5)$$

I and J label the sites $(-1,0), (0,1)$ and $(0,-1)$ directly coupled to $\mathbf{0}$ for $\sigma_{\mathbf{0}}$, and the sites $(2,0), (1,1)$ and $(1,-1)$

directly coupled to **1** for $\sigma_{\mathbf{1}}$. For each tip position and different energies $E \leq E_F$, the Green's functions of the right strip determining $\sigma_{\mathbf{1}}$ are calculated using recursive Green's function (RGF) algorithm (see Ref. [9] and references therein).

The self-energies $\Sigma^{\rm H}_{\mathbf{0}}$ and $\Sigma^{\rm H}_{\mathbf{1}}$ describe the Hartree corrections yielded by the inter-site repulsion U to the potentials of the sites **0** and **1** respectively, while the Fock self-energy $\Sigma^{\rm F}$ modifies the hopping term t_d because of exchange. The matrix elements $(G_{\rm nano}(E))_{i,j}$ $(i,j=0,1)$ being given by Eq. (3), the HF self-energies are the self-consistent solution of 3 coupled integral equations:

$$\Sigma^{\rm H}_{\mathbf{0}} = -\tfrac{U}{\pi}\Im\int_{-\infty}^{E_F}(G_{\rm nano}(E))_{1,1}dE \quad (6)$$

$$\Sigma^{\rm H}_{\mathbf{1}} = -\tfrac{U}{\pi}\Im\int_{-\infty}^{E_F}(G_{\rm nano}(E))_{0,0}dE \quad (7)$$

$$\Sigma^{\rm F} = \tfrac{U}{\pi}\Im\int_{-\infty}^{E_F}(G_{\rm nano}(E))_{0,1}dE. \quad (8)$$

The imaginary parts of the above integrals are equal to zero for $E<-4$. For $-4<E<E_F$, the poles on the real axis make necessary to integrate Eqs. (6-8) using Cauchy theorem. We have used a semi-circle centered at $(E_F-4)/2$ in the upper part of the complex plane. The integration is done using the Gauss–Kronrod algorithm. This requires to calculate $G_{\rm nano}$ (and therefore $\sigma_{\mathbf{0}}(z)$ and $\sigma_{\mathbf{1}}(z,V_T)$) for a sufficient number (≈ 100) of complex energies z on the semi-circle, before determining the self-consistent solutions of Eqs. (6- 8) recursively. Calculating $\sigma_{\mathbf{1}}(z,V_T)$ for each tip position (r_T,θ_T), one can obtain the 2d images giving $\Sigma^{\rm HF}$ as a function of the tip position.

Once the self-energies $\Sigma^{\rm HF}$ are obtained in the zero temperature limit, the interacting nanosystem is described by an effective one body Green's function, identical to the one of a non interacting nanosystem, with potentials $V_G+\Sigma^{\rm H}_{\mathbf{0}}$ and $V_G+\Sigma^{\rm H}_{\mathbf{1}}$ and hopping $-t_d+\Sigma^{\rm F}$. Then, the many channel Landauer-Buttiker formula $g=$ trace $tt^\dagger$ valid for non interacting systems can be used to obtain the zero temperature conductance g in units of e^2/h (for polarized electrons). This conductance corresponds to a measure made between the two ohmic contacts sketched in FIG. 1. We use the RGF algorithm to obtain the Green's function of the measured system, from which the transmission matrix t can be expressed [14].

For having negligible lattice effects and SGM images characteristic of the continuum limit, we consider a low filling factor $\nu\approx 1/25$ in the 2d strips, corresponding to a Fermi energy (momentum) $E_F=-3.57$ ($k_F=0.668$). The width of the strip ($2L_y+1=301$) is sufficient for having a 2d behavior in the vicinity of the nanosystem. Moreover, we take small values of the nanosystem hopping t_d, in order to increase [12, 13] the effect of the tip upon the HF self-energies. In FIG. 2 (lower right), the conductance g_0 without tip ($V_T=0$) is given as a function of the gate potential V_G for increasing values of U. When t_d is small, the double peak structure of $g_0(V_G)$ characteristic of a nanosystem with two sites merges [13] to form a single peak. Hereafter, the SGM images are given for a gate potential $V_G^*(U)$ for which $g_0(V_G)$ is maximum.

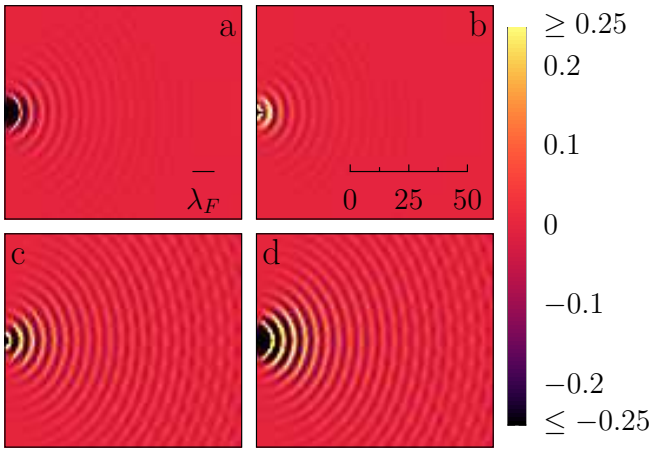

FIG. 3: Images obtained by scanning the tip ($V_T=-2$) on the right strip. The Fermi wave length λ_F and the scale are given in FIG. (a) and (b). Upper part: Relative corrections $\delta\Sigma^{\rm F}/\Sigma^{\rm F}(V_T=0)$ (FIG. a) and $\delta\Sigma^{\rm H}_{\mathbf{0}}/\Sigma^{\rm H}_{\mathbf{0}}(V_T=0)$ (FIG. b) of the Fock and Hartree self-energies as a function of the tip position for $U=1.7$. $\delta\Sigma=\Sigma(V_T=-2)-\Sigma(V_T=0)$. $\Sigma^{\rm F}(V_T=0)=-0.120$ and $\Sigma^{\rm H}_{\mathbf{0}}(V_T=0)=0.529$.Lower part: Relative corrections $\delta g/g_0$ as a function of the tip position for $U=0$ (FIG. c) and $U=1.7$ (FIG. d). Used parameters: $E_F=-3.57$, $t_d=0.01$ and strips of width $2L_y+1=301$. $V_G=V_G^*=-2.870$ (-2.187) and $g_0=0.188$ (0.0014) for $U=1.7$ ($U=0$).

The effect of the tip upon $\Sigma^{\rm F}$ and $\Sigma^{\rm H}_{\mathbf{0}}$ is shown as a function of the tip position (x_T,y_T) in the upper part of FIG. 3. The images show fringes spaced by $\lambda_F/2$ which fall off as $1/r_T^2$. In FIG. 4 (upper left), the Fock term $\Sigma^{\rm F}$ is plotted as a function of r_T for $\theta_T=0$. The decay can be described by a $\cos(2k_Fr_T+\delta)/r_T^2$ fit. Similar fits characterize the 2 Hartree terms. Since the effect of the tip upon $\Sigma^{\rm H}_{\mathbf{0}}$ is driven by Friedel oscillations, $\Sigma^{\rm H}_{\mathbf{0}}$ decays as 2d Friedel oscillations. $\Sigma^{\rm H}_{\mathbf{1}}$ and $\Sigma^{\rm F}$ have similar decays.

In the lower part of FIG. 3, the effect of the tip upon the conductance is given as a function of (x_T,y_T). The left figure gives $\delta g/g_0$ without interaction ($U=0$), where $\delta g=g(V_T=-2)-g_0$. One can see that δg decays as r_T increases, the image exhibiting fringes spaced by $\lambda_F/2$. The decay depends on the angle θ_T. For $\theta_T=0$, $\delta g(U=0)$ falls off as $1/r_T$, and not as $1/r_T^2$ (isotropic assumption). This is shown in FIG. 4 (upper right), a fit of the form $a_1\cos(2k_Fr_T+\delta_1)/r_T$ describing the decay.

In FIG. 3 (d), $\delta g/g_0$ is shown when the electrons interact inside the nanosystem ($U=1.7$). The interation effect $\propto 1/r_T^2$ of the tip upon g via $\Sigma^{\rm HF}(V_T)$ enhances the fringes near the nanosystem. Since the SGM images exhibit fringes spaced by $\lambda_F/2$, decaying as $1/r_T^2$ for $\Sigma^{\rm HF}$ and as $1/r_T$ for g when $U=0$, we fit the effect of the tip

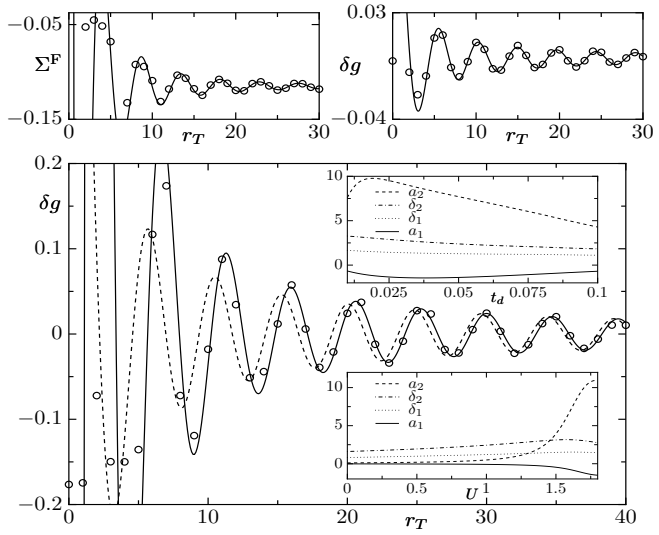

FIG. 4: Effect of the tip as a function of r_T for $\theta_T = 0$ when $E_F = -3.57$, $2L_y + 1 = 301$ and $V_T = -2$. Upper left: $1/r_T^2$ decay of the Fock self-energy $\Sigma^{\rm F}$ ($\circ$) for $U = 1.7$. Solid line: $-0.115 + 2.379\cos(2k_F r_T + 0.765)/r_T^2$. Same parameters as in FIG. 3 (a). Upper right: $1/r_T$-decay of δg for $U = 0$ and $t_d = 0.1$, $g_0 = 0.133$, $V_G^* = -2.187$. Solid line: $0.110\cos(2k_F r_T - 1.2)/r_T$. Lower part: $1/r_T^2$-decay of δg ($\circ$) at small distances r_T induced by an interaction $U = 1.7$ when $t_d = 0.01$ ($g_0 = 0.188$). Fit $F(r_T)$ with $a_1 = -0.676$, $a_2 = -7.605$, $\delta_1 = 1.664$ and $\delta_2 = 0.120$ (solid line). Taking $a_2 = 0$ in $F(r_T)$ (dashed line) fails to describe δg at small distances r_T, and does not matter at large distances r_T. Insets: Parameters of $F(r_T)$ fitting δg as a function of t_d when $U = 1.7$ (upper inset) and as a function of U when $t_d = 0.02$ (lower inset).

upon g when $U \neq 0$ by a function

$$F(r_T) = \frac{a_1 \cos(2k_F r_T + \delta_1)}{r_T} + \frac{a_2 \cos(2k_F r_T + \delta_2)}{r_T^2} \quad (9)$$

which contains 4 adjustable parameters a_1, δ_1, a_2 and δ_2. The $\cos(2k_F r_T + \delta)$ terms give the fringes. The $1/r_T$ term fits the decay without interaction. The $1/r_T^2$ term is added for taking into account the effect of the tip upon g occurring near the nanosystem via $\Sigma^{\rm HF}$.

When r_T is large, the effect of the tip upon $\Sigma^{\rm HF}$ is negligible and $\delta g(r_T)$ falls off as when $U = 0$ ($1/r_T$ decay). As r_T varies, a crossover from a decay described by the term $a_2 \cos(2k_F r_T + \delta_2)/r_T^2$ of $F(r_T)$ towards a decay described by $a_1 \cos(2k_F r_T + \delta_1)/r_T$ takes place. This is shown in FIG. 4 (lower part), where $a_2 \neq 0$ is necessary for describing $g(r_T)$ at small distances r_T. This crossover is accompanied by a phase shift of the fringes ($\delta_2 \neq \delta_1$), which can be seen in the figure. To find this crossover, we have studied how the 4 parameters of $F(r_T)$ depend on t_d and on U (insets of FIG. 4). To get a $1/r_T^2$ decay which persists in a large domain around the nanosystem, one needs $|a_2| \gg |a_1|$. This occurs for small t_d (upper inset) and $U > 1$ (lower inset).

In summary, neglecting electron-electron interactions and disorder in the strips, we have shown that the SGM images allow to measure the interaction strength inside the nanosystem. From zero temperature transport measurements, one can detect a $1/r_T^2$ decay of the SGM images around the nanosystem, and via $a_2(U)$, the value of U characteristic of the nanosystem can be determined. For observing this $1/r_T^2$ decay, one needs (i) large electron-electron interactions inside the nanostructure (sufficient r_s factor), (ii) large density oscillations induced by the tip (V_T large), and (iii) that those oscillations modify the density inside the nanostructure (r_T not too large, strong coupling between the nanostructure and the strips).

We thank S. N. Evangelou for useful comments and a careful reading of the manuscript. The support of the network "Fundamentals of nanoelectronics" of the EU (contract MCRTN-CT-2003-504574) is gratefully acknowledged.

* Present address: Department of Physics, University of Ioannina, Ioannina 45 110, Greece

[1] M. A. Topinka, B. J. LeRoy, R. M. Westervelt, S. E. J. Shaw, R. Fleischmann, E. J. Heller, K. D. Maranowski, and A. C. Gossard, Nature **410**, 183 (2001).
[2] M. A. Topinka, B. J. LeRoy, S. E. J. Shaw, E. J. Heller, R. M. Westervelt, K. D. Maranowski, and A. C. Gossard, Science **289**, 2323 (2000).
[3] N. Aoki, A. Burke, C. R. da Cunha, R. Akis, D. K. Ferry, and Y. Ochiai, J. Phys.: Conf. Series **38**, 79 (2006).
[4] M. P. Jura, M. A. Topinka, L. Urban, A. Yazdani, H. Shtrikman, L. N. Pfeiffer, K. W. West, and D. Goldhaber-Gordon, Nature **3**, 841 (2007).
[5] F. Martins, B. Hackens, M. G. Pala, T. Ouisse, H. Sellier, X. Wallart, S. Bollaert, A. Cappy, J. Chevrier, V. Bayot, et al., Phys. Rev. Lett. **99**, 136807 (2007).
[6] M. T. Woodside and P. L. McEuen, Science **296**, 1098 (2002).
[7] A. Pioda, S. Kicin, T. Ihn, M. Sigrist, A. Fuhrer, K. Ensslin, A. Weichselbaum, S. E. Ulloa, M. Reinwald, and W. Wegscheider, Phys. Rev. Lett. **93**, 216801 (2004).
[8] E. J. Heller, K. E. Aidala, B. J. LeRoy, A. C. Bleszynski, A. Kalben, R. M. Westervelt, K. D. Maranowski, and A. C. Gossard, Nano Lett. **5**, 1285 (2005).
[9] G. Metalidis and P. Bruno, Phys. Rev. B **72**, 235304 (2005).
[10] K. J. Thomas, J. T. Nicholls, M. Y. Simmons, M. Pepper, D. R. Mace, and D. A. Ritchie, Phys. Rev. Lett. **77**, 135 (1996).
[11] Y. Asada, A. Freyn, and J.-L. Pichard, Eur. Phys. J. B **53**, 109 (2006).
[12] A. Freyn and J.-L. Pichard, Phys. Rev. Lett. **98**, 186401 (2007).
[13] A. Freyn and J.-L. Pichard, Eur. Phys. J. B **58**, 279 (2007).
[14] S. Datta, *Electronic Transport in Mesoscopic Systems* (Cambridge University Press, 1997).